REPORT DOCUMENTATION PAGE

Form Approved OMB No. 0704-0188

1. AGENCY USE ONLY (Leave blank)	2. REPORT DATE	3. REPORT TYPE AND DATES COVERED
	1999	Final Report

4. TITLE AND SUBTITLE

High-Power Diffraction-Limited Diode Lasers Using Self-Adaptive Resonator Design

5. FUNDING NUMBERS

F617089

6. AUTHOR(S)

Dr. Michael J. Damzen

7. PERFORMING ORGANIZATION NAME(S) AND ADDRESS(ES)

Imperial College of Science, Technology, and Medicine
The Blacklett Lab., Prince Consort Rd.,
London SW7 2BZ
England

8. PERFORMING ORGANIZATION REPORT NUMBER

N/A

9. SPONSORING/MONITORING AGENCY NAME(S) AND ADDRESS(ES)

EOARD
PSC 802 BOX 14
FPO 09499-0200

10. SPONSORING/MONITORING AGENCY REPORT NUMBER

SPC 98-4021

11. SUPPLEMENTARY NOTES

12a. DISTRIBUTION/AVAILABILITY STATEMENT

Approved for public release; distribution is unlimited.

12b. DISTRIBUTION CODE

A

13. ABSTRACT (Maximum 200 words)

This report results from a contract tasking Imperial College of Science, Technology, and Medicine as follows: The contractor will investigate the feasibility of obtaining diffraction-limited beam quality from high-power semiconductor amplifier devices by incorporating a novel self-adaptive resonator design.

14. SUBJECT TERMS

EOARD, Diode lasers

15. NUMBER OF PAGES

19

16. PRICE CODE

N/A

17. SECURITY CLASSIFICATION OF REPORT	18. SECURITY CLASSIFICATION OF THIS PAGE	19. SECURITY CLASSIFICATION OF ABSTRACT	20. LIMITATION OF ABSTRACT
UNCLASSIFIED	UNCLASSIFIED	UNCLASSIFIED	UL

NSN 7540-01-280-5500

Standard Form 298 (Rev. 2-89)
Prescribed by ANSI Std. 239-18
298-102

FINAL REPORT

USAF Contract No: F61775-98-WE014

SPC 98-4021

High-Power, Diffraction-limited Diode Lasers

Using

Self-Adaptive Resonator Design

Principal Investigator: Dr Michael J. Damzen
The Blackett Laboratory,
Imperial College,
London SW7 2BZ,U.K.
Tele:(+44) 171 594 7783;
Fax: (+44) 171 594 7744;
e-mail: m.damzen@ic.ac.uk

A. INTRODUCTION:

High-power diode lasers have very poor spatial coherence and undesirably high beam divergence (e.g. 20W diode bars have beam quality M^2-factor > 1000). This is due to the need to scale to large emitter dimensions to prevent facet damage which occur at output power densities of about ~ 10-20mW/μm of emitter dimension. Broad area structures typically operate with a highly multimode spatial output with added problems of beam filamentation associated with a number of physical features of the diode device (e.g. linewidth enhancement factor, thermal lensing and localised device defects). The achievement of high-power, diffraction-limited (M^2~1) beam quality, direct from diode laser devices, would be a major technological breakthrough for many applications that require low divergence or high focusability, whilst also offering high efficiency, and economies in cost, weight and size compared to equivalent diode-pumped or flashlamp-pumped solid-state laser devices.

We report in this document a theoretical feasibility study for obtaining diffraction-limited beam quality from high-power semiconductor amplifier devices by incorporating a novel self-adaptive resonator technology. The adaptive technology of this proposal is one that has been pioneered at Imperial College for use in solid-state lasers and are to be transferred to the specific problems involved in high-power diode laser media and their specific associated architectures.

The ***project objectives*** were:
1. To assess the feasibility of using a self-adaptive resonator in broad area diode amplifiers.
2. To determine the conditions for obtaining diffraction-limited high-power diode radiation.

As stated in our original proposal, these objectives were to be accomplished by numerical simulation of the resonator with the following ***work programme*** steps:
1. Formulation of nonlinear equations for diode saturation and grating formation;
2. Writing numerical code for simulation of adaptive diode laser resonator;
3. Consideration of efficiency and phase shift of gratings and frequency chirping effects in the resonator dynamics;
4. Establish optimum diode parameters for efficient operation;
5. Consider geometrical issues of resonator architecture.

B. CONCEPT OF THE SELF-ADAPTIVE RESONATOR

The self-adaptive gain-grating resonator concept

The resonator incorporates a gain-medium in a self-intersecting loop geometry (see Figure 1). Consider beam A_1 that propagates around the loop and accumulates the phase distortions of the amplifiers (thermal and modal scrambling) and those of any other intracavity element. The resultant distorted loop beam A_3 forms an interference pattern with beam A_1 that modulates the inversion of the gain medium (by gain saturation), forming a ***gain volume 'hologram' that encodes the distortion***. The gain hologram acts as a ***diffraction grating*** that, with sufficient gain, allows the build-up of a backward ring resonator mode (beams A_2 and A_4) that reconstructs the hologram. This produces a self-reproducing spatial mode that is a ***phase conjugate*** of the input beam A_1 and corrects for beam distortions in the resonator,

such that the backward oscillation through the distortions of the loop can lead to a diffraction-limited output. The resonator can work in two modes of operation. One is with an external laser providing the injection source of the input beam A_1. The second mode (the self-starting adaptive oscillator as shown in Figure 1) is without an external injection but by using an output coupler (with reflectivity R_{OC}) as a feedback source and the onset of grating formation is from spontaneous emission. In reality, there are up to four-gain gratings from each interacting beam pair in the amplifier. A near unidirectional device (incorporating a Faraday rotator, [e.g. see ref. 5]) provides a different forward transmission (T_+) to backward transmission (T_-) and ensures efficient energy extraction in the output coupler direction. At Imperial College, we have demonstrated the effectiveness of this concept [e.g. ref. 1-5] with the maintenance of TEM_{oo} operation through distortions in pulsed flashlamp-pumped Nd:YAG amplifiers and in the tuneable lasing medium Ti:sapphire. We have also shown that this technique leads to single-longitudinal-mode operation due to the Bragg-selectivity of the gratings and coherent writing condition, as well as leading to high-peak-power, self-Q-switched pulses (500mJ, 10ns).

With regard to this contract it was proposed to consider this resonator architecture for use with a broad-area diode amplifier to achieve high-power and near diffraction-limited output. The diode amplifier provides some new features in the design of this laser architecture. The diode system will be able to operate in the continuous-wave mode (unlike previous experimental demonstrations with pulsed systems), and the gain grating will have a strong phase component due to the linewidth enhancement factor in diode lasers that relates to the refractive index change with carrier inversion density. In addition, there are the specific geometrical issues of the highly-asymmetric diode gain region that require consideration of methods for efficient beam overlap. As the evaluation of this system was proposed to be by numerical modelling, it was necessary, as a first step, to develop the theoretical analysis and numerical codes that were appropriate to the diode gain medium.

C. THEORETICAL ANALYSIS of DIODE GAIN-GRATINGS

Rate Equation for the laser gain coefficient

The appropriate equation for the evolution of the gain coefficient in a four-level laser system is given by

$$\frac{\partial \alpha(\underline{r},t)}{\partial t} = R(t) - \frac{1}{U_S} I_T(\underline{r},t).\alpha(\underline{r},t) - \frac{\alpha(\underline{r},t)}{\tau_\ell} \qquad (1)$$

where $\alpha(t)$ is the amplitude gain coefficient, $I_T(t)$ is the total optical intensity, $R(t)$ is a pumping term which generates the gain, $U_S = h\nu/\sigma$ is the saturation fluence of the medium and τ_ℓ is the gain (or upper-state) lifetime, h is Planck's constant, ν is the laser frequency and σ is the stimulated emission cross-section. On the right hand side of equation 1, the first term is a rate of pumping the inversion, the second is the stimulated emission rate and the third is the spontaneous emission rate. In a semiconductor diode amplifier the gain coefficient is complex having real (pure gain) and imaginary (refractive index) parts. While the gain coefficient can generally have a dispersive (refractive index) component due to operation at a wavelength away from gain line-centre of the lasing transition, semiconductor lasers also have an additional, much stronger, refractive index contribution. It is convenient to describe this refractive index component with the incorporation of the **linewidth enhancement factor**

β such that $\alpha = \alpha_g(1 + i\beta)$ and where α_g is the (real) gain coefficient and β specifying the relative contribution of the refractive index change with inversion density. A typical value for $|\beta|$ in semiconductors is 5.

Equation 1 can be recast as

$$\tau_\ell \frac{\partial \alpha(\underline{r},t)}{\partial t} = \tau_\ell R(t) - \left(1 + \frac{I_T(\underline{r},t)}{I_S}\right).\alpha(\underline{r},t) \tag{2}$$

where I_S is the saturation intensity of the medium given by $I_S = U_S/\tau_\ell$. As described later, it is convenient in the analysis to quote intensities normalised to the saturation intensity.

Optical Field Equations

The total intensity in the medium is given by $I_T = |E_T|^2$ where E_T is the total field in the medium which, if four optical fields are present, can be written as

$$\underline{E}_T = \sum_{j=1}^{4} \underline{A}_j e^{-i\underline{k}_j \cdot \underline{r}} \tag{3}$$

where we consider the four-wave mixing (FWM) geometry of Figure 1 with pairs of fields taken to be counter-propagating to each other. When the total field, together with the appropriate atomic polarisation for the lasing species ($P_{at} = \varepsilon_0 \chi E = -i\varepsilon_0(2\alpha/k)E$), is substituted into the nonlinear Maxwell wave equation (with plane wave and slowly-varying envelope approximations) the following coupled wave equations are obtained for the optical field amplitudes

$$\begin{aligned} \left((-1)^{j+1}\frac{\partial}{\partial z} + \frac{n}{c}\frac{\partial}{\partial t}\right)\underline{A}_j(\underline{r},t) &= +\left(\alpha.\underline{E}_T.e^{+i\underline{k}_j.\underline{r}}\right)_j \qquad j = 1 \rightarrow 4 \\ &= \textstyle\sum_{k=1}^{4} \kappa_{jk} A_k \end{aligned} \tag{4}$$

where selection of the appropriate phase-matched components in the $\alpha.\underline{E}_T$ source term leads to the FWM coupling coefficients κ_{jk}, and α is a function of field amplitudes and determined by solution of equation 2.

In the general case, there are four induced gain-gratings due to interference of pairs of beams. For the sake of simplicity, we consider the single transmission grating case when, for example, the interacting fields are such that $\underline{A}_1$ and $\underline{A}_3$ are co-polarised but with orthogonal polarisation state (or different frequency) to $\underline{A}_2$ and $\underline{A}_4$ which are also co-polarised. The resulting normalised intensity pattern is given by

$$\begin{aligned} \frac{I_T(\underline{r},t)}{I_S} &= \sigma_i + |\tau_i|\cos\left(K_\tau x - \phi_\tau\right) \\ &= \sigma_i + \tfrac{1}{2}\left(\tau_i e^{-iK_\tau x} + \tau_i^* e^{+iK_\tau x}\right) \end{aligned} \tag{5}$$

$$\sigma_i = \frac{1}{I_s}\sum_{j=1}^{4} A_j(\underline{r},t).A_j^*(\underline{r},t) \tag{6a}$$

$$\tau_i = |\tau_i| e^{+i\phi_\tau} = \frac{2}{I_s}\left[A_1.A_3^* + A_2^*.A_4\right] \tag{6b}$$

where $K_\tau x = \underline{k}.(\underline{r}_1 - \underline{r}_3)$ is the fast spatially-varying phase of the interference pattern (taken to be in the direction x which is normal to the bisector of beams A_1 and A_3) and σ_i and τ_i are the average (d.c.) and modulated components, respectively, of the intensity pattern and normalised to the saturation intensity I_s.

In the steady-state regime $\left(\partial/\partial t \to 0\right)$ the solution to equation 1 and 2 can be written as

$$\alpha = \frac{\tau_\ell R}{1 + I_T/I_S} = \frac{\alpha_0}{1 + I_T/I_S} \tag{7}$$

where α_0 is the (unsaturated) small-signal gain coefficient. When the interference pattern of equation 5 is substituted for I_T, a gain grating is written of the form

$$\begin{aligned} \alpha &= \frac{\alpha_0}{1 + \sigma_i + |\tau_i| \cos\left(K_\tau x - \phi_\tau\right)} \\ &= \frac{\Gamma_0}{1 + M_\tau \cos\left(K_\tau x - \phi_\tau\right)} \end{aligned} \tag{8}$$

where Γ_0 and M_τ are the incoherently saturated gain coefficient and a modulation parameter, respectively, and are given by

$$\Gamma_0(z) = \frac{\alpha_0}{1 + \sigma_i(z)} \tag{9a}$$

$$M_\tau(z) = \frac{|\tau_i(z)|}{1 + \sigma_i(z)} \tag{9b}$$

The periodic modulation of the gain coefficient described by equation 8 can be expanded in a Fourier cosine series as follows

$$\begin{aligned} \alpha(x,z) &= \sum_{n=0}^{\infty} \alpha_\tau^{(n)}(z) \cos\left[n\left(K_\tau x - \phi_\tau\right)\right] \\ &= \tfrac{1}{2} \sum_{n=0}^{\infty} \alpha_\tau^{(n)}(z) e^{-in\left(K_\tau x - \phi_\tau\right)} + \textbf{c.c.} \end{aligned} \tag{10}$$

with coefficients given by

$$\alpha^{(0)}(z) = +\frac{\Gamma_0}{\sqrt{1 - M_\tau^2}} \tag{11a}$$

$$\alpha^{(n)}(z) = (-1)^n \frac{2\Gamma_0}{\sqrt{1 - M_\tau^2}} \left(\frac{1 - \sqrt{1 - M_\tau^2}}{M_\tau}\right)^n \tag{11b}$$

The substitution of equation 10 into equation 4 and the selection of the appropriate phase-matched components lead to the following set of coupled equations describing the steady-state FWM interaction

$$+\frac{dA_1}{dz} = \gamma A_1 + \kappa_\tau A_3 \tag{12a}$$

$$-\frac{dA_2}{dz} = \gamma A_2 + \kappa_\tau^* A_4 \tag{12b}$$

$$+\frac{dA_3}{dz} = \gamma A_3 + \kappa_\tau^* A_1 \tag{12c}$$

$$-\frac{dA_4}{dz} = \gamma A_4 + \kappa_\tau A_2 \tag{12d}$$

with coupling coefficients

$$\gamma(z) = \alpha_\tau^{(0)}(z) = +\frac{\Gamma_0}{\sqrt{1-M_\tau^2}} \tag{13a}$$

$$\kappa_\tau(z) = \frac{1}{2}\alpha_\tau^{(1)}(z)\, e^{+i\phi_\tau} = -\frac{\Gamma_0}{M_\tau}\left(\frac{1}{\sqrt{1-M_\tau^2}} - 1\right) e^{+i\phi_\tau} \tag{13b}$$

A further useful point to note is that manipulation of the system of equations 12 yields the following conserved quantity for the steady-state FWM interaction.

$$A_1(z).A_2(z) + A_3(z).A_4(z) = \text{constant} \tag{14}$$

The set of equation 12 are the key system equations that need to be numerically solved to simulate the diode saturation and grating formation in a FWM geometry and with appropriate boundary conditions for simulation of adaptive loop resonators.

The formulated nonlinear optical equations described above are for steady-state conditions which apply for interaction times >> laser inversion lifetime (~ nanosecond in semiconductors) and should be a valid approximation for most practical scenarios. [We have also derived a corresponding set of transient equations but their limit of validity will probably not be relevant to diode laser simulations (unless ultrashort pulse formation occurs).] The equations allow for a general saturable inversion where changes in inversion lead to changes in both gain and refractive index (via the linewidth enhancement factor). The linewidth enhancement factor β (ratio of change of real to imaginary susceptibility with inversion density N) is necessary to be incorporated in real semiconductor amplifiers. When $\beta = 0$ we have the pure gain case, when $\beta > 1$ the phase grating is stronger than the gain grating. Since typically in semiconductor amplifier devices $|\beta| \sim 5$, this effect cannot be neglected as the refractive index is the dominant grating component.

D. Numerical Modelling Results

A numerical code has been written that solves the coupled nonlinear equations (equations 12) and simulates a four-wave mixing interaction geometry in the diode amplifier.

D.1 Diffraction Efficiency of a Semiconductor Gain Grating

D.1.1 High diffraction efficiency. As a first step, we considered the writing of a grating with a pair of strong (saturating) beams (A_1 and A_3 as in Figure 1) and probed the diffraction efficiency of this grating with a weak (non-saturating) Bragg-matched third beam (A_2). We have plotted a set of graphs of diffraction efficiency ($\eta = |A_4/A_2|^2$) versus writing beam intensity ($I_w=I_1=I_3$) for a range of linewidth enhancement factor ($\beta = 0 - 5$). An example of the numerically computed diffraction efficiency versus writing intensity is shown in Figure 2. We consider the case of a small-signal amplifier gain of 100.

We find as a rule (for this case of equal writing beams) that the diffraction efficiency is enhanced by a factor of $(1 + \beta^2)$ compared to the pure gain ($\beta=0$) case. Hence for a typical semiconductor ($\beta\sim5$) we expect an increase in diffraction efficiency by a factor ~26 compared to the pure gain case ($\beta=0$). We observe in Figure 2 a diffraction efficiency value of approximately 50 for the $\beta=5$ case (N.B. diffraction efficiency = 50 not 50%.). The greater than unity diffraction efficiency is physically possible due to the gain seen by the probing and diffracted beams in the amplifier unit. This enormous diffraction efficiency is a very positive result since it indicates that a semiconductor adaptive resonator should be very efficient even at moderate small-signal gain levels compared to a pure gain ($\beta=0$) amplifier.

D.1.2 Intensity-dependent phase shift. The intensity-dependent change in the average refractive index of the gain medium (due to the linewidth enhancement factor) leads to an intensity-dependent phase shift of each interacting beam on propagating through the gain medium. This effect does not adversely affect the diffraction efficiency for the above case modelled, as evidenced by the high diffraction efficiency results. It is expected, however, that this phase-shift will have an important effect in the adaptive resonator since the resonant oscillation condition of laser action demands a correct phasing of the lasing mode.

D.2 Injected Self-Adaptive Laser Resonator

We have converted the numerical code for simulation of an adaptive resonator with the diode amplifier in a self-intersecting loop geometry with a single-frequency injection beam provided by an external source (e.g. low-power single-mode diode laser). Self-interference of the input beam in the saturable diode amplifier results in the modulation of the inversion density leading to backward oscillation of radiation in a 'ring-resonator' via diffraction from the inversion grating.

D.2.1 Good efficiency of laser oscillation. Figure 3 illustrates results of the numerical simulations of the adaptive resonator. Figure 3a shows the output intensity as a function of input intensity in an amplifier (small-signal gain = 400) with different values of linewidth enhancement factor ($\beta=0,1,5$) and a non-reciprocal transmission element in the loop with forward transmission factor of 5%. The set of graphs in Figure 3a show that high values of β produce a significant decrease in threshold and increase in output efficiency compared to the pure gain case. For $\beta = 5$, the extraction efficiency is almost 50% without optimisation of the loop transmission factor. Figure 3b shows the corresponding reflectivity (ratio of output intensity to input intensity) as a function of input intensity, showing very high values of reflectivity are expected (several thousand times). It is noted that the simulations model a single transmission grating. In reality, if all beams are coherent there will also be further enhancement in the efficiency from the reflection grating e.g. formed by interference between beams A_2 and A_3. The efficiency is estimated to be greater than 75% with the combined

grating. With higher gain efficiency could approach nearer the 90% level. This estimate is however complicated by the fact that the oscillation mode is frequency-shifted from the input mode, so further modelling would be required to better quantify the issue of efficiency.

D.2.2 Frequency-shift of Oscillating Mode. The other key feature predicted in the simulations is a small frequency shift of the output beam (A_2) compared to the input (from the external injection source) by some fraction of a cavity mode spacing (c/L where c is speed of light and L is loop length). This is illustrated in Figure 4 showing a plot of frequency shift with β parameter. The exact value of this frequency shift depends on the value of β and input intensity and is due to the phase of the grating relative to the optical interference pattern and the intensity-dependent phase shifts experienced by the beams when $\beta > 0$ (see Section D.1.2). In the above analysis, it is assumed that there is no non-reciprocal phase shift in the resonator loop. (In practice, it is possible to construct a non-reciprocal phase shift by appropriate use of a Faraday rotator element).

D.3 The Self-Starting adaptive laser oscillator

The injected self-adaptive resonator only requires a low power seeding (A_1) to generate an intense oscillation and output beam A_2. In this respect, the injection source is only a small fraction of the power of the whole system, thereby causing little decrease of efficiency by its inclusion. The extra simplicity of the self-starting system may however be attractive, removing the need for the seeder source and also issues of decoupling feedback into the injection source.

We numerically modelled the self-starting adaptive laser resonator with the feedback output coupler mirror, and initiation would be by spontaneous emission.

D.3.1 Output Intensity and Efficiency. Figures 5,6 and 7 show output intensity from the self-starting resonator for small-signal gain of 400 and for the cases β=0, β=1 and β=5, respectively. In each graph the output intensity is normalised to the saturation intensity and plotted as a function of output coupler reflectivity (R_{OC}) and intracavity forward transmission factor (T_+). To allow the system to oscillate resonantly it was assumed that we could incorporate into the loop a non-reciprocal phase element that could bring the forward and backward modes into frequency degeneracy.

From the sequence of Figures 5-7, it is seem that the maximum output intensity increases with β with values I/I_s = 1.2 (β=0), 1.6 (β=1) and 3.1 (β=5). These correspond to extraction efficiencies of 20% (β=0), 27% (β=1) and 52% (β=5). With a multi-grating analysis, these values will increase as with the injected adaptive resonator case. A most interesting, and perhaps surprising, result is seen in Figure 7. The output intensity is only weakly sensitive to forward transmission factor (T_+) and mainly is controlled by the output coupler reflectivity. Most significantly the output intensity with $T_+ = 1$ can be close to the maximum output intensity with the correct range of output coupler reflectivity. This is not the case for the β=0 amplifier medium as shown in Figure 5, which shows the output intensity is very sensitive to T_+ and output coupler reflectivity. The difference is probably due to the β=5 case operates with a medium that can have significantly higher diffraction efficiency and operates much higher above threshold. The significance of the high output obtainable with T_+=1 (and T_-=1) suggests that it is possible to efficiently operate the resonator without the non-reciprocal transmission element, whereas in the β=0 case it is needed to maintain $T_+ << 1$ and T_-=1. This would greatly

simplify the resonator architecture and even allow the possibility of making the resonator monolithic.

E. Geometrical Issues

A remaining consideration for the diode resonator design is the geometrical problems of efficiently launching beams into the diode amplifier, including one beam at a small angle to form the spatial grating modulation for the resonator concept. This is an optical design exercise. Since launching into diode amplifiers has been performed successfully in prior systems, it seems reasonable to expect the adaptive resonator geometry will be practical to construct. Clearly, a full 3-D model with diffraction and transverse effects would be interesting to verify numerically the ability of the self-adaptive system to preserve diffraction-limited beam quality through the broad-area diode amplifier. This code however involves considerable computational power and time and was not possible within the time-frame of this contract.

F. CONCLUSIONS

We have successfully completed the work programme of our original proposal. We have formulated the nonlinear equations of beam interaction in a diode amplifier, we have written the numerical code to simulate the adaptive resonator and our simulation results have informed us about the behaviour of an adaptive resonator, in both the injected and self-starting modes of operation.

Some key conclusions are summarised below:

- The linewidth enhancement factor of semiconductor laser amplifiers leads to inversion gratings with very high diffraction efficiencies that can be one or two orders of magnitude higher than in a pure gain medium.
- There are intensity-dependent phase shifts associated with the saturation of the inversion in a diode amplifier that lead to the output frequency of the injected resonator being shifted from that of the input frequency.
- The power efficiency of both the injected and self-starting adaptive resonator is shown to be greater than 50% for a single grating analysis, but a multi-grating analysis suggests that much higher efficiencies are possible.
- Our results suggest that it will be possible to operate the resonator efficiently without need for the non-reciprocal transmission element. This is a very new result for the diode amplifier, and is not possible for efficient operation with the pure gain amplifier. This result reduces significantly the complexity for construction of this adaptive architecture.
- The self-starting adaptive resonator system has the problem of requiring an intracavity non-reciprocal phase shifting element to maintain the cavity on resonance. (Further analysis would be required to see what happens without the "phase-shifter".)
- The injected adaptive resonator system does not need a phase-shifting device if a small frequency shift in the output (compared to the injecting input) is acceptable.
- Diode amplifiers have been used in the past so the main additional consideration for the adaptive resonator concept is the injection into the amplifier of an additional beam at small angle to the input beam. This may be awkward due to the high asymmetry of the diode amplifier, but is expected to be physically achievable.

RECOMMENDATION

The most promising route to obtaining high power, diffraction-limited diode radiation is by using the injected adaptive resonator. The injection source would be a single-mode diode laser but would only need to be a low-power device (<1% of the output power of the required amplifier source). The injection diode would determine the wavelength of the system. The results of our analysis indicate that the resonator can be operated efficiently without requiring the non-reciprocal transmission element and that makes the technology most practical.

G. REFERENCES

[1] M.J. Damzen, R.P.M. Green and K.S. Syed, "Self-adaptive solid-state laser oscillator formed by dynamic gain-grating holograms", Opt. Lett., 20, 1704 (1995)

[2] R.P.M. Green et al, "Holographic laser oscillator which adaptively corrects for polarisation and phase distortions", Phys. Rev. Lett., 77, 3533 (1996)

[3] K.S. Syed, et al, "Transient modelling of pulsed phase conjugation experiments in a saturable Nd:YAG amplifier", Opt.Commun., 112, 175 (1994)

[4] R.P.M. Green et al, "Phase conjugate reflectivity and diffraction efficiency of gain gratings in Nd:YAG", Opt. Commun., 102, 288 (1993)

[5] O.Wittler et al. "Characterisation of a distortion-corrected Nd:YAG laser with a self-conjugating loop geometry", IEEE J. Quantum Electron., 35, 656 (1999)

CAPTIONS FOR FIGURES

Figure 1. Self-adaptive resonator design. Illustrated is the self-intersecting loop geometry in a diode amplifier with gain (G_0), with formation of a diffractive inversion-grating, incorporation of a non-reciprocal transmission element (NRTE), and beam notation (A_1-A_4). Injected adaptive resonator uses an external seeding of beam A_1 (and without output coupler mirror). Self-starting adaptive resonator uses output coupler with reflectivity R_{OC}, as shown.

Figure 2. Diffraction efficiency (η) of an optically-induced inversion grating in a diode amplifier as a function of (equal) writing beam intensity (I/I_s) for various linewidth enhancement factors (β).

Figure 3. Numerical results of a) the output intensity (I_2/I_s) and b) the reflectivity (I_2/I_1) as a function of input intensity (I_1/I_s) and for different linewidth enhancement factors (β) for the case of the injected adaptive laser resonator.

Figure 4. Frequency-shift, as a fraction of half the loop mode spacing (c/2L), of the output of the injected adaptive laser resonator relative to the input frequency.

Figure 5. Output intensity (I/I_s) of the self-starting adaptive laser resonator as a function of the output coupler reflectivity (R_{OC}) and forward loop transmission (T_+). Linewidth enhancement factor β=0.

Figure 6. As in Figure 5, but with linewidth enhancement factor β=1.

Figure 7. As in Figure 5, but with linewidth enhancement factor β=5.

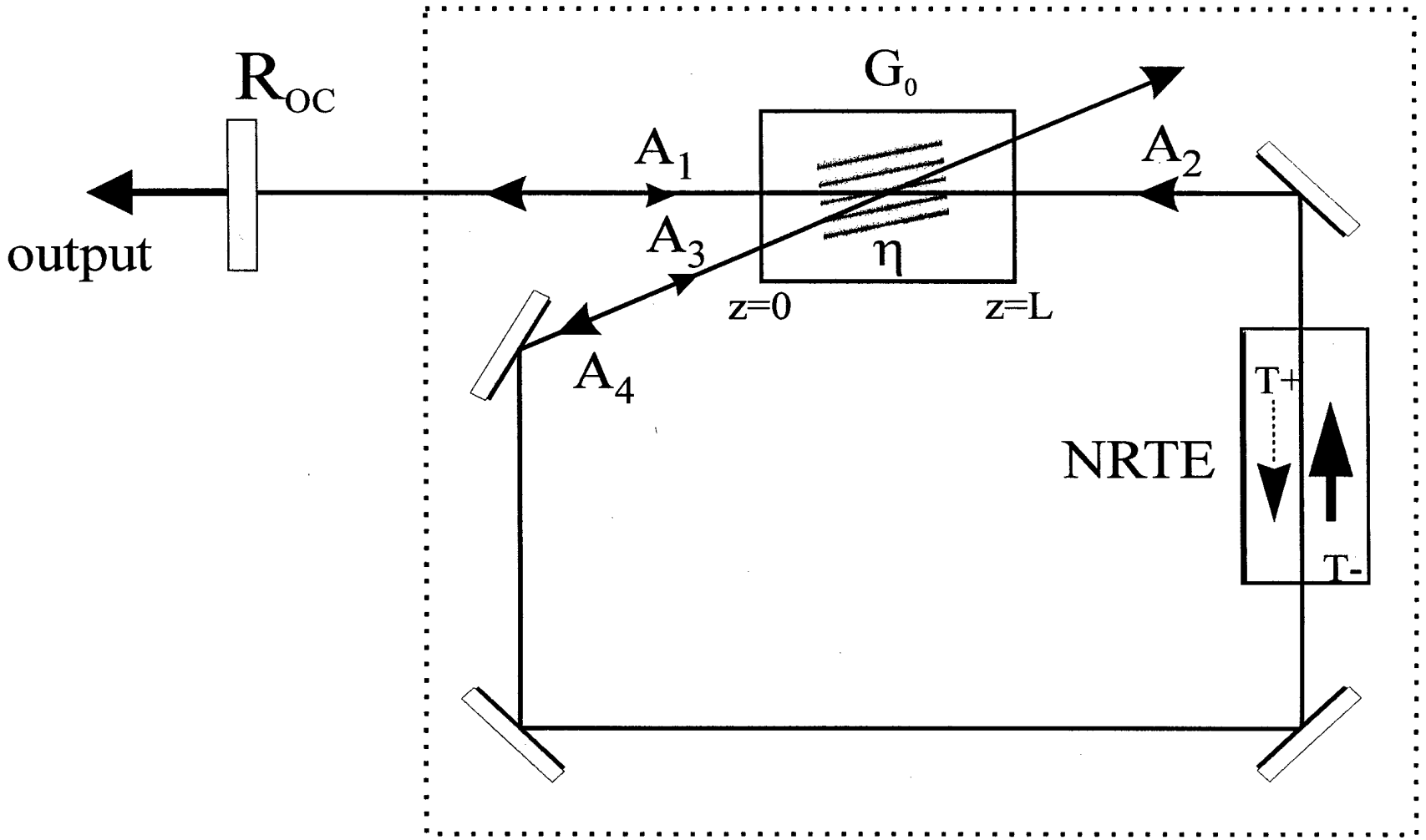

Figure 1

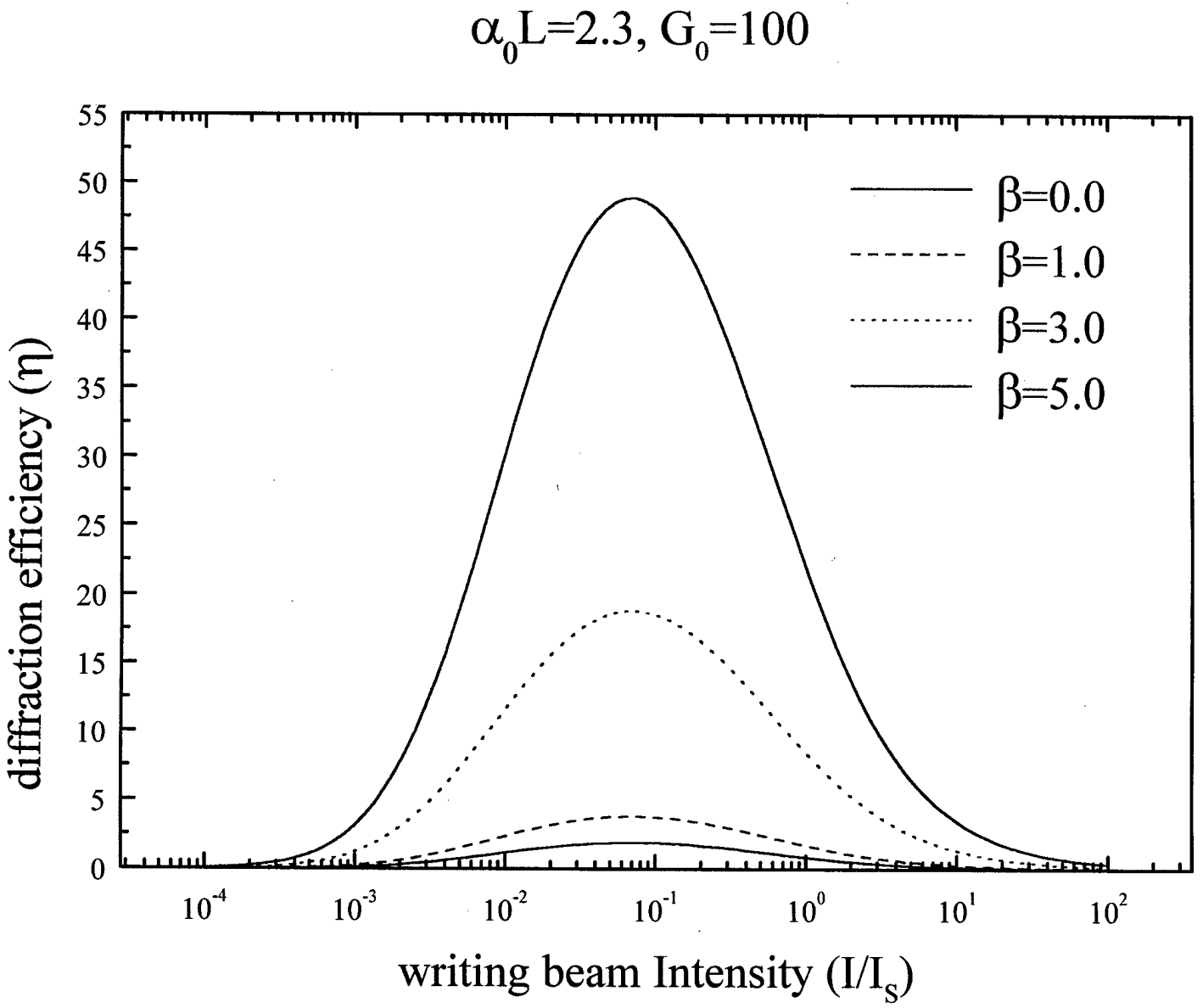
$\alpha_0 L=2.3$, $G_0=100$
diffraction efficiency (η)
writing beam Intensity (I/I_S)
β=0.0
β=1.0
β=3.0
β=5.0
0
5
10
15
20
25
30
35
40
45
50
55
10^{-4}
10^{-3}
10^{-2}
10^{-1}
10^{0}
10^{1}
10^{2}

Figure 2

[a]

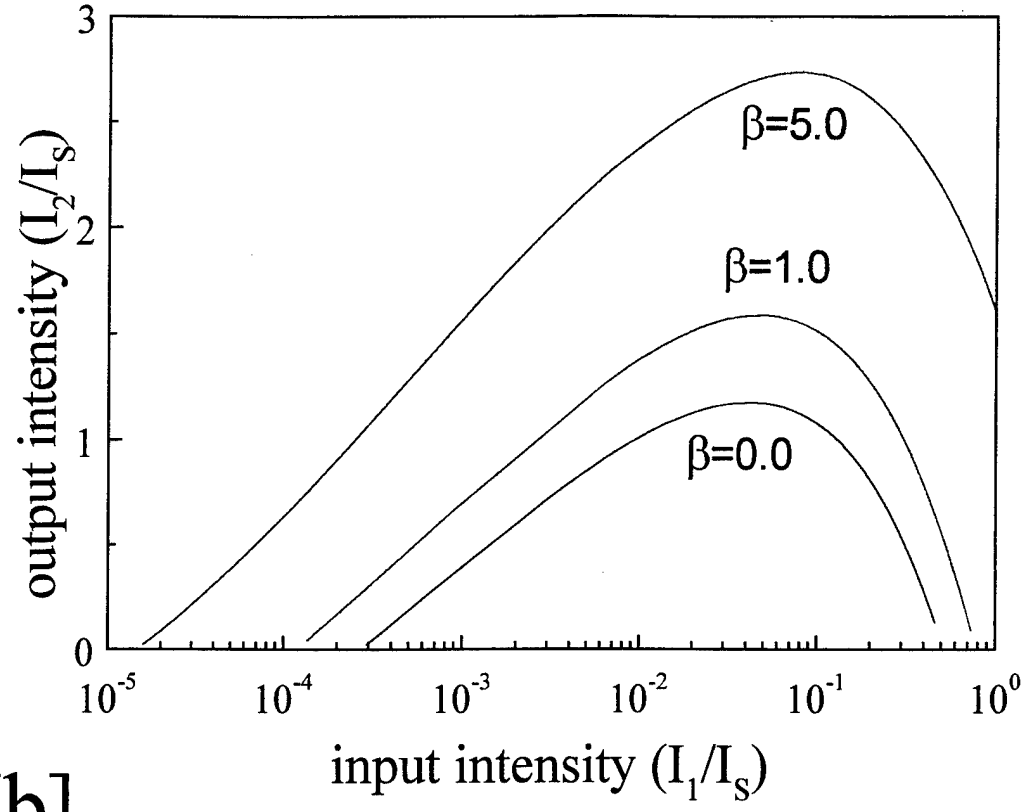
3
2
1
0
output intensity (I_2/I_S)
β=5.0
β=1.0
β=0.0
10^{-5}
10^{-4}
10^{-3}
10^{-2}
10^{-1}
10^{0}
input intensity (I_1/I_S)

[b]

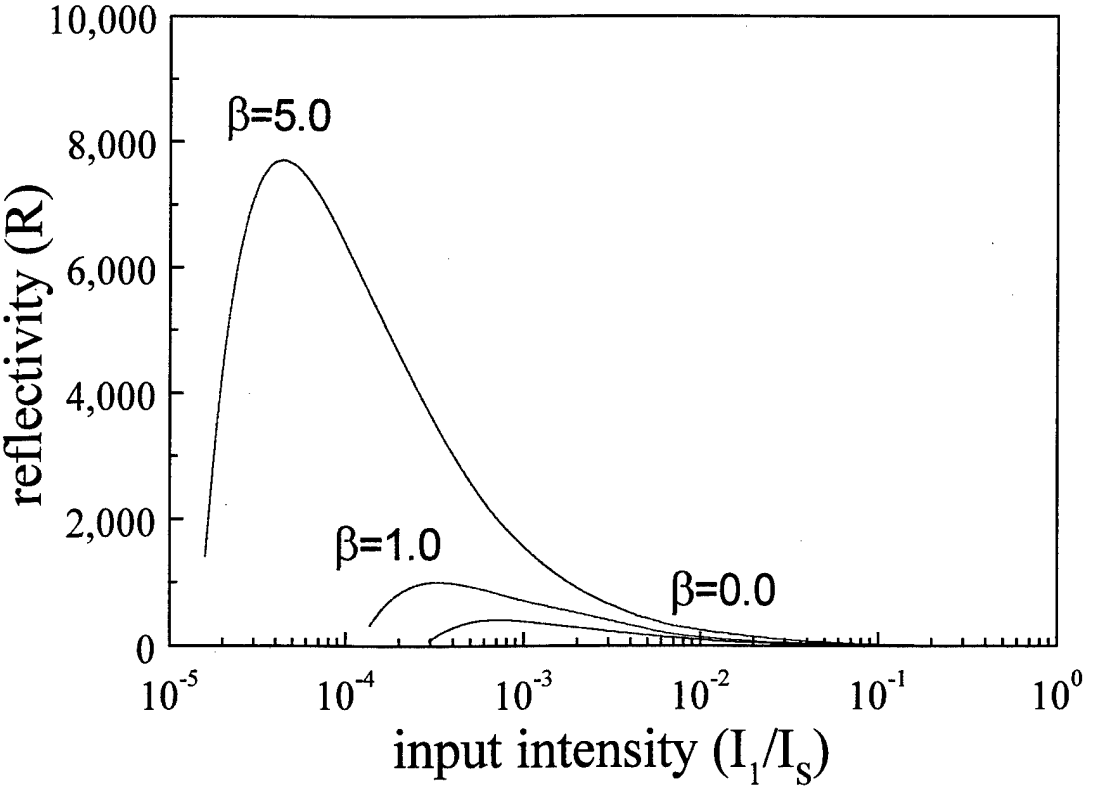
10,000
8,000
6,000
4,000
2,000
0
reflectivity (R)
β=5.0
β=1.0
β=0.0
10^{-5}
10^{-4}
10^{-3}
10^{-2}
10^{-1}
10^{0}
input intensity (I_1/I_S)

Figure 3

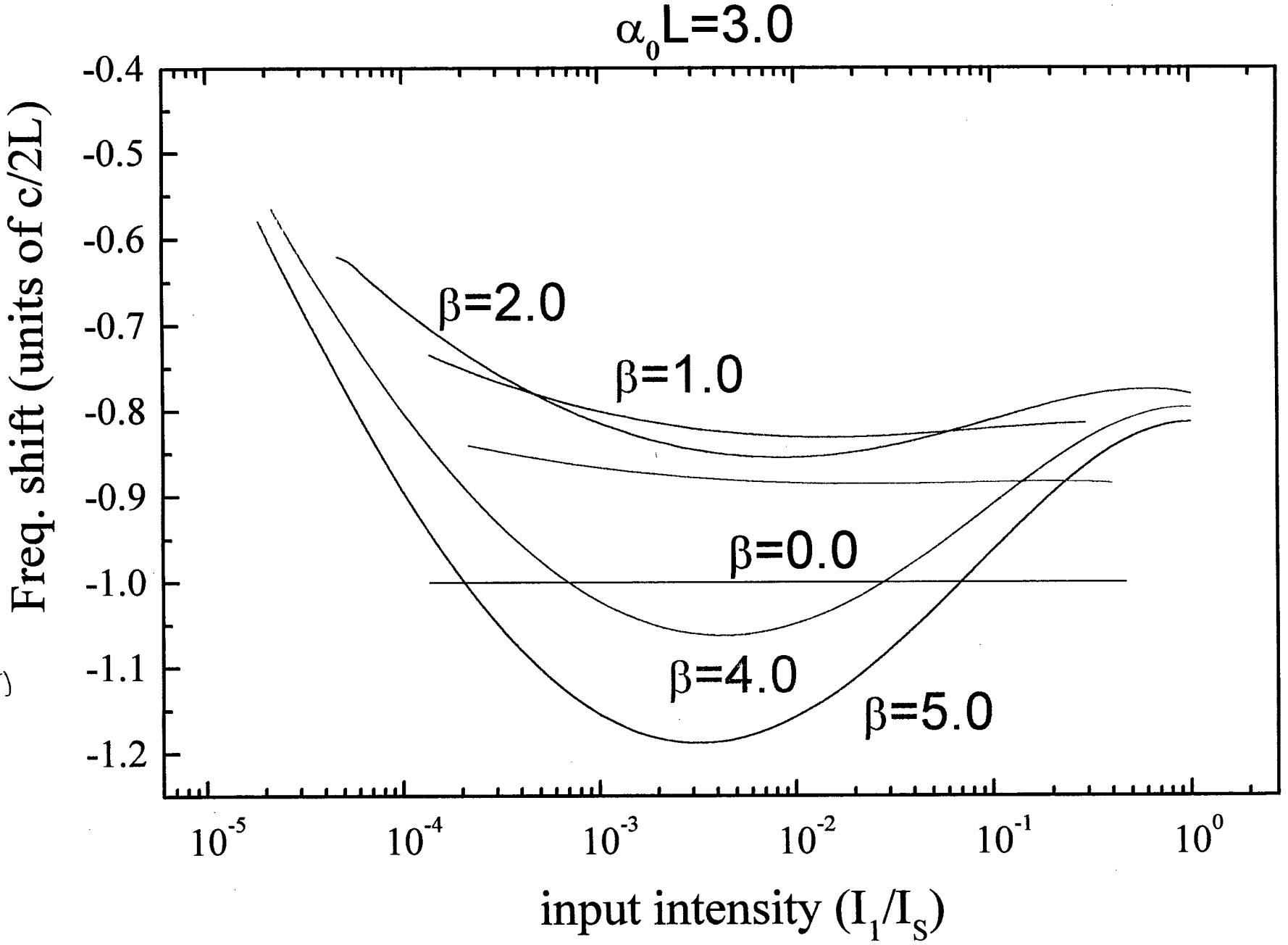
$\alpha_0 L=3.0$
Freq. shift (units of c/2L)
-0.4
-0.5
-0.6
-0.7
-0.8
-0.9
-1.0
-1.1
-1.2
β=2.0
β=1.0
β=0.0
β=4.0
β=5.0
10^{-5}
10^{-4}
10^{-3}
10^{-2}
10^{-1}
10^{0}
input intensity (I_1/I_S)

Figure 4.

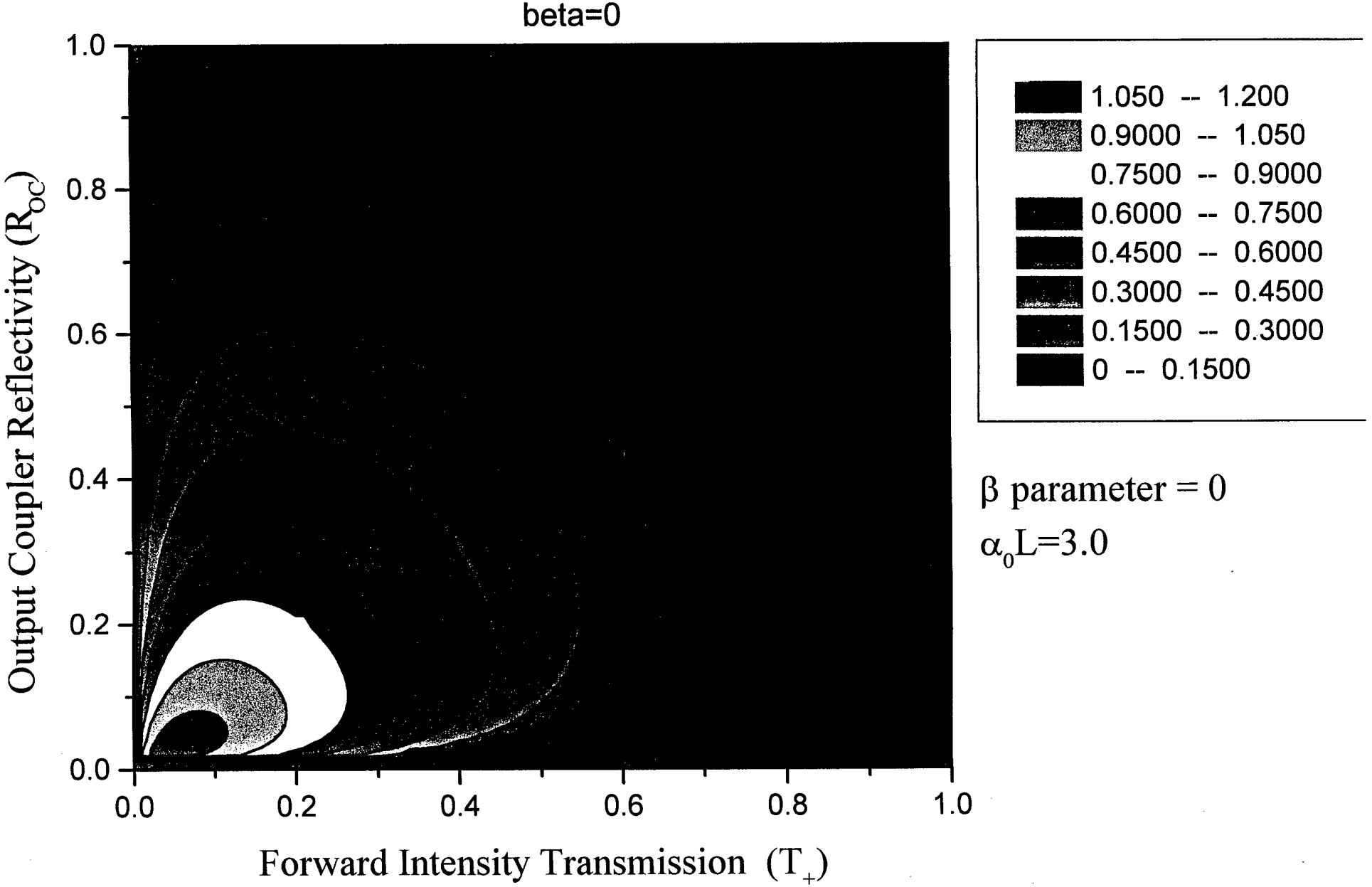
beta=0
1.050 -- 1.200
0.9000 -- 1.050
0.7500 -- 0.9000
0.6000 -- 0.7500
0.4500 -- 0.6000
0.3000 -- 0.4500
0.1500 -- 0.3000
0 -- 0.1500
β parameter = 0
$\alpha_0 L$=3.0
Output Coupler Reflectivity (R_{OC})
Forward Intensity Transmission (T_+)
0.0
0.2
0.4
0.6
0.8
1.0

Figure 5

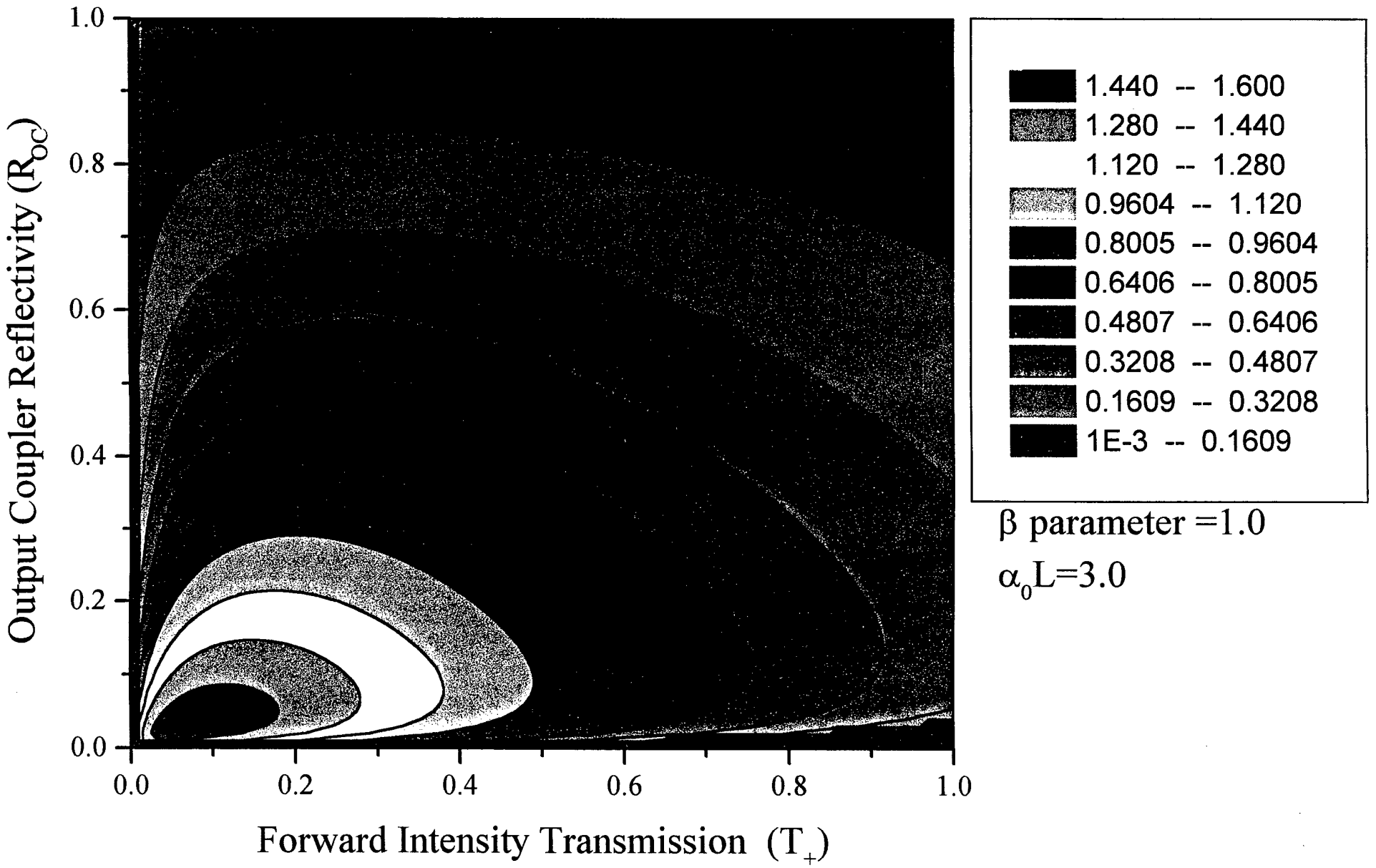
1.0
0.8
0.6
0.4
0.2
0.0
0.0
0.2
0.4
0.6
0.8
1.0
Output Coupler Reflectivity (R_{OC})
Forward Intensity Transmission (T_+)
1.440 -- 1.600
1.280 -- 1.440
1.120 -- 1.280
0.9604 -- 1.120
0.8005 -- 0.9604
0.6406 -- 0.8005
0.4807 -- 0.6406
0.3208 -- 0.4807
0.1609 -- 0.3208
1E-3 -- 0.1609
β parameter =1.0
$\alpha_0 L$=3.0

Figure 6

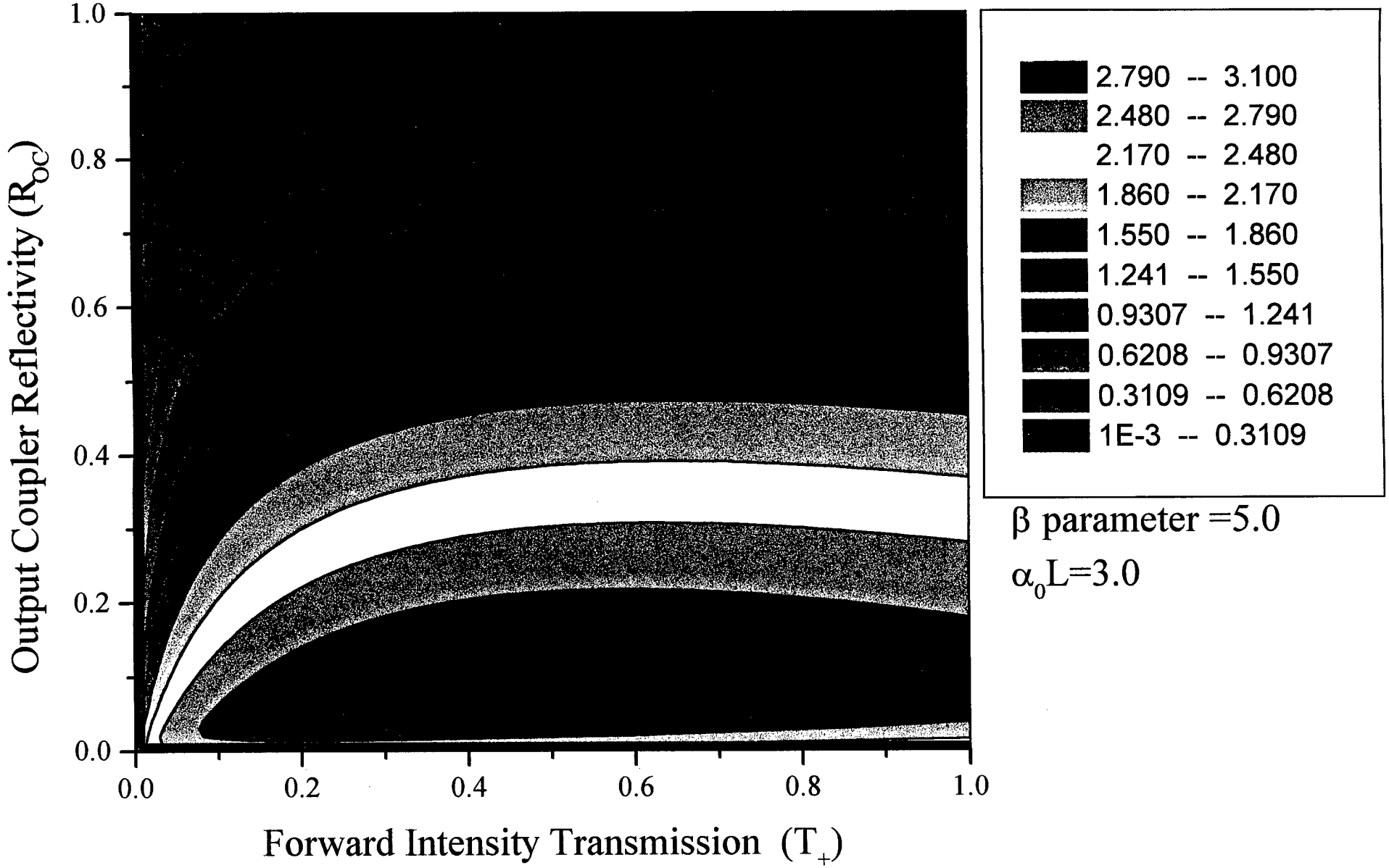
Output Coupler Reflectivity (R_{OC})
1.0
0.8
0.6
0.4
0.2
0.0
0.0
0.2
0.4
0.6
0.8
1.0
Forward Intensity Transmission (T_+)
2.790 -- 3.100
2.480 -- 2.790
2.170 -- 2.480
1.860 -- 2.170
1.550 -- 1.860
1.241 -- 1.550
0.9307 -- 1.241
0.6208 -- 0.9307
0.3109 -- 0.6208
1E-3 -- 0.3109
β parameter =5.0
$\alpha_0 L$=3.0

Figure 7